Comparison of several maneuvering target tracking models

Article *in* Proceedings of SPIE - The International Society for Optical Engineering · July 1998

DOI: 10.1117/12.327127

CITATIONS
22

READS
4,150

2 authors:

Gregory A. Mcintyre
Applied Research Associates, Inc.
18 PUBLICATIONS **394** CITATIONS
SEE PROFILE

Kenneth Hintz
George Mason University
78 PUBLICATIONS **1,082** CITATIONS
SEE PROFILE

A comparison of several maneuvering target tracking models

Gregory A. McIntyre[a] and Kenneth J. Hintz[b]

[a] Department of Operational Sciences, Air Force Institute of Technology
[b] Department of Electrical and Computer Engineering, George Mason University

ABSTRACT

The tracking of maneuvering targets is complicated by the fact that acceleration is not directly observable or measurable. Additionally, acceleration can be induced by a variety of sources including human input, autonomous guidance, or atmospheric disturbances. The approaches to tracking maneuvering targets can be divided into two categories both of which assume that the maneuver input command is unknown. One approach is to model the maneuver as a random process. The other approach assumes that the maneuver is not random and that it is either detected or estimated in real time. The random process models generally assume one of two statistical properties, either white noise or an autocorrelated noise. The multiple-model approach is generally used with the white noise model while a zero-mean, exponentially correlated acceleration approach is used with the autocorrelated noise model. The nonrandom approach uses maneuver detection to correct the state estimate or a variable dimension filter to augment the state estimate with an extra state component during a detected maneuver.

Another issue with the tracking of maneuvering target is whether to perform the Kalman filter in Polar or Cartesian coordinates. This paper will examine and compare several exponentially correlated acceleration approaches in both Polar and Cartesian coordinates for accuracy and computational complexity. They include the Singer model in both Polar and Cartesian coordinates, the Singer model in Polar coordinates converted to Cartesian coordinates, Helferty's third order rational approximation of the Singer model and the Bar-Shalom and Fortmann model. This paper shows that these models all provide very accurate position estimates with only minor differences in velocity estimates and compares the computational complexities of the models.

Keywords: tactically maneuvering targets, Kalman filters, target tracking, exponentially correlated acceleration models

1. BACKGROUND

Tracking a maneuvering target involves filtering and prediction in order to track the target. "*Filtering* refers to estimating the state vector at the current time, based upon all past measurements. *Prediction* refers to estimating the state at a future time; we shall see that prediction and filtering are closely related."[1] One of the most commonly used technique for target tracking is the discrete Kalman filter developed by Rudolf Kalman. The Kalman filter is "*the*" optimal linear, unbiased state estimator given its assumptions and is used to filter past measurements and predict where a target will be in the future. This target location prediction is then used to aim a sensor in order to track the target. An error covariance matrix is maintained as part of the normal computation process of the Kalman filter. This error covariance matrix can be considered as a measure of uncertainty of the kinematic state (called the state estimate) of the target.

The tracking of maneuvering targets may be complicated by the fact that acceleration may not be directly observable or measurable. Additionally, apparent acceleration can be induced by a variety of sources including human input, autonomous guidance, or atmospheric disturbances. Several approaches to tracking maneuvering targets have been proposed in the literature and can be divided into two categories both of which assume that the maneuver input command is unknown. One approach is to model the maneuver as a random process. The other approach assumes that the maneuver is not random and that it is either detected or estimated in real time. Both assume a rectilinear model of target track. The random process models generally assume one of two statistical properties, either white noise or an autocorrelated noise. The multiple-model approach is generally used with the white noise model while a zero-mean, exponentially correlated acceleration approach is used with the autocorrelated noise model. The nonrandom approach uses maneuver detection to correct the state estimate or a variable dimension filter to augment the state estimate with an extra state component during a detected maneuver.[2]

Further author information —
G.Mc.: Email: gmcintyr@afit.af.mil: Telephone: 937-255-6565x4323; Fax 937-656-4943
K.J.H.: Email: khintz@gmu.edu; WWW: http://fame.gmu.edu/~khintz; Telephone 703-993-1592; Fax 703-993-1601

Another issue to be considered when tracking a maneuvering target is whether to perform the Kalman filter in Polar or Cartesian (x, y) coordinates. In general, a sensor's measurements are reported in range and bearing (or bearing only in the cases of passive sensors) to the target. If Cartesian coordinate are used, then the range (r) and bearing (θ) measurements must be converted through the transformation equations:

$$x = r\cos\theta \qquad (1)$$
$$y = r\sin\theta$$

which results in cross-correlated measurement noise. The resulting covariance matrix can be represented as

$$\mathbf{R}_{xy} = \begin{bmatrix} \sigma_x^2 & \sigma_{xy}^2 \\ \sigma_{xy}^2 & \sigma_y^2 \end{bmatrix} \qquad (2)$$

by using a first order expansion[3,4,5] where

$$\sigma_x^2 = \sigma_r^2\cos^2\theta + r^2\sigma_\theta^2\sin^2\theta \qquad (3)$$
$$\sigma_y^2 = \sigma_r^2\sin^2\theta + r^2\sigma_\theta^2\cos^2\theta$$
$$\sigma_{xy}^2 = \tfrac{1}{2}\sin\theta(\sigma_r^2 - r^2\sigma_\theta^2)$$
$$\sigma_r^2 = \text{range measurement variance}$$
$$\sigma_\theta^2 = \text{bearing measurement variance}$$

In using Cartesian coordinates, the state equation is linear while the corresponding measurement equation is nonlinear. Using Polar coordinates, the state equation is nonlinear but the measurement equation is linear.[6] This means that tracking in Cartesian coordinates has the advantage that it allows the use of linear target dynamic models for extrapolation while Polar coordinates may lead to more complicated extrapolation. By examining (1) and (2), using Cartesian coordinates for tracking leads to two major disadvantages. The first is that the measured (or estimated) range must be available while the second is that measurement errors are coupled.

The exponentially correlated acceleration model approach is one of the approaches most widely used to track maneuvering targets. This paper examines and compares several exponentially correlated acceleration approaches in both Polar and Cartesian coordinates for accuracy and computational complexity. The paper is organized as follows. The next section describes the models that will be used in the comparisons. The results of the comparisons are presented in Section 3 while Section 4 provides a summary of our comparisons.

2. MODEL DESCRIPTIONS

Several exponentially correlated acceleration models and a constant velocity model are described in this section. They include the Singer model in both Polar and Cartesian coordinates, the Sklansky model (the constant velocity model), Helferty's third-order rational approximation of the Singer model, and the Bar-Shalom and Fortmann model.

2.1 Singer model using Polar coordinates

Singer[7,8,9] developed a model that incorporates the maneuver capability of a target that is not only simple but also suitably represents the maneuver characteristics. The Singer model for manned maneuvering targets assumes that a target normally moves at constant velocity and that turns, evasive maneuvers, and accelerations due to atmospheric disturbances can be viewed as perturbations of the constant velocity trajectory. These accelerations are termed target maneuvers and are correlated in time with the previous time or the next time increment. That is to say that if a target is maneuvering at time t, it is likely to be maneuvering at time $t+\tau$ assuming that τ is sufficiently small. Singer[7] states that a lazy turn will give correlated inputs for up to one minute, evasive maneuvers due to radar detection, terrain features, or preprogrammed maneuvers will provide correlated inputs for 10 to 30 seconds, and atmospheric turbulence for only 1 to 2 seconds. Due to this time dependence, the maneuvers are neither additive nor Gaussian. Singer's probability density function for a target's maneuvers are shown in Figure 1. This distribution is based on the assumption that a target can[7]:

- Accelerate (maneuver) at its maximum rate, $\pm A_{max}$ with a probability of P_{max}
- No maneuver with a probability of P_0, or
- Maneuver between $-A_{max}$ and $+A_{max}$ according to the uniform distribution shown in Figure 1.

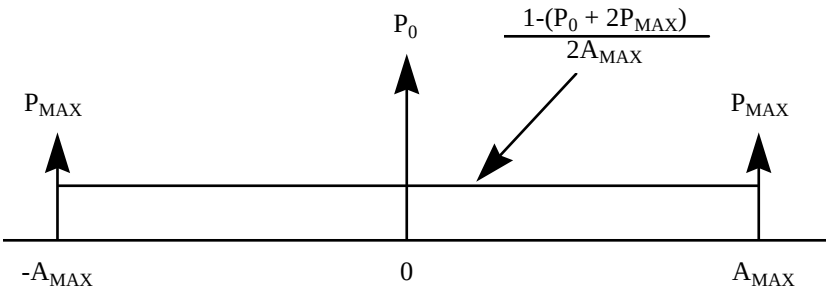

Figure 1: Target maneuver probability density function [8]

In order to use this model in a optimal filter such as a Kalman filter, the maneuver noise needs to be whitened. Singer[8] uses a procedure analogous to the whitening procedure developed by Wiener and Kolmogorov. The whitening processes is done by augmenting the state vector to include the maneuver variables and expressing them recursively in terms of white noise.

The target maneuver model is in Polar coordinates and given by the state equation

$$\mathbf{x}_{k+1} = \Phi\, \mathbf{x}_k + \mathbf{G}\, \mathbf{u}_k \qquad (4)$$

where

$$\mathbf{x}_k = \begin{bmatrix} r_k & \dot{r}_k & u_{r,k} & \theta_k & \dot{\theta}_k & u_{\theta,k} \end{bmatrix}^T$$

$$\mathbf{w}_k = \begin{bmatrix} w_{1,k} & w_{2,k} \end{bmatrix}^T$$

$$\Phi = \begin{bmatrix} 1 & T & 0 & 0 & 0 & 0 \\ 0 & 1 & 1 & 0 & 0 & 0 \\ 0 & 0 & \rho & 0 & 0 & 0 \\ 0 & 0 & 0 & 1 & T & 0 \\ 0 & 0 & 0 & 0 & 1 & 1 \\ 0 & 0 & 0 & 0 & 0 & \rho \end{bmatrix} \qquad \mathbf{G} = \begin{bmatrix} 0 & 0 \\ 0 & 0 \\ 1 & 0 \\ 0 & 0 \\ 0 & 0 \\ 0 & 1 \end{bmatrix}$$

$T =$ sampling period

$\rho =$ correlation coefficient of maneuver

$= e^{\alpha T}$ or $\cong 1 - \alpha T$ if αT is small

$$\mathbf{Q}_k = E\left[\mathrm{w}_k w_k^T\right] = \begin{bmatrix} \sigma_{M_1}^2 (1-\rho) & 0 \\ 0 & \sigma_{M_2}^2 (1-\rho) \end{bmatrix}$$

$$\sigma_{M_1}^2 = \frac{A_{\max}^2 T^2}{3}\left(1 + 4P_{\max} - P_0\right)$$

$$\sigma_{M_2}^2 = \frac{A_{\max}^2 T^2}{3R}\left(1 + 4P_{\max} - P_0\right)$$

$\mathbf{R} =$ target range

The measurement equation is given by

$$\mathbf{z}_k = \mathbf{H}\, \mathbf{x}_k + \mathbf{v}_k \qquad (5)$$

where

$$\mathbf{H} = \begin{bmatrix} 1 & 0 & 0 & 0 & 0 & 0 \\ 0 & 0 & 0 & 1 & 0 & 0 \end{bmatrix}$$

$$\mathbf{R}_k = \begin{bmatrix} \sigma_{r,k}^2 & 0 \\ 0 & \sigma_{\theta,k}^2 \end{bmatrix}$$

The standard filter equations for state estimation extrapolation, error covariance extrapolation, Kalman gain matrix computation, state estimate update, and error covariance updates are then applied. The filter is initialized based on the first two observations with the state estimate given by

$$\hat{x}_2 = \begin{bmatrix} z_2(1) & \frac{1}{T}\left(z_2(1) - z_1(1)\right) & 0 & z_2(2) & \frac{1}{T}\left(z_2(2) - z_1(2)\right) & 0 \end{bmatrix}^T \quad \textbf{(6)}$$

and the nonzero elements of the updated error covariance matrix, P_2^+, defined as

$$\begin{aligned} P_{11} &= \sigma_r^2 & P_{44} &= \sigma_\theta^2 \\ P_{22} &= \sigma_{M_1}^2 + \left(\frac{2\sigma_r^2}{T^2}\right) & P_{55} &= \sigma_{M_2}^2(1) + \left(\frac{2\sigma_\theta^2}{T^2}\right) \\ P_{33} &= \sigma_{M_1}^2 & P_{66} &= \sigma_{M_2}^2(1) \\ P_{12} &= P_{21} = \frac{\sigma_r^2}{T^2} & P_{45} &= P_{54} = \frac{\sigma_\theta^2}{T^2} \\ P_{23} &= P_{32} = \rho\sigma_{M_1}^2 & P_{56} &= P_{65} = \rho\sigma_{M_2}^2(1) \end{aligned} \quad \textbf{(7)}$$

with σ_{M_1} calculated in (4) and

$$\sigma_{M_2}^2(1) = \frac{\sigma_{M_1}^2}{z_1^2(1)} \quad \textbf{(8)}$$

2.2 Singer model using Cartesian coordinates

A version of the Singer model can be developed for Cartesian coordinates using a constant velocity model with exponentially correlated acceleration. The state equation and measurement model is

$$\begin{aligned} \dot{\mathbf{x}}(t) &= \mathbf{F}(t)\,\mathbf{x}(t) + \mathbf{G}(t)\,\mathbf{w}_1(t) \\ \mathbf{z}(t) &= \mathbf{H}(t)\,\mathbf{x}(t) + \mathbf{v}(t) \end{aligned} \quad \textbf{(9)}$$

where

$$\mathbf{x}(t) = \begin{bmatrix} x(t) & \dot{x}(t) & y(t) & \dot{y}(t) \end{bmatrix}^T$$

$$\mathbf{F}(t) = \begin{bmatrix} 0 & 1 & 1 & 0 \\ 0 & 0 & 0 & 0 \\ 0 & 0 & 0 & 1 \\ 0 & 0 & 0 & 0 \end{bmatrix}$$

$$\mathbf{G}(t) = \begin{bmatrix} 0 & 0 \\ 1 & 0 \\ 0 & 0 \\ 0 & 1 \end{bmatrix}$$

$$\mathbf{H}(t) = \begin{bmatrix} 1 & 0 & 0 & 0 \\ 0 & 0 & 1 & 0 \end{bmatrix}$$

where the process noise is exponentially correlated, assumed to be equally distributed in the *x* and *y* directions, and used to model the target acceleration. The measurement noise is normally distributed with zero mean and covariance **R** as in (2). The process noise can be whitened by augmenting the state vector by appending the necessary state vector components of a linear shaping filter. This results in a linear model driven by white noise. This whitening process is described in Grewal and Andrews[10] and repeated below. Modeling the correlated noise, $\mathbf{w}_1(t)$, in (9) with a shaping filter yields

$$\dot{\mathbf{x}}_{SF}(t) = \mathbf{F}_{SF}(t)\,\mathbf{x}_{SF}(t) + \mathbf{G}_{SF}(t)\,\mathbf{w}_2(t) \qquad \mathbf{w}_2(t) = \mathbf{H}_{SF}(t)\,\mathbf{x}_{SF}(t) \qquad \textbf{(10)}$$

where *SF* denotes the shaping filter and $\mathbf{w}_2(t)$ is a zero mean white Gaussian noise. Using the system model given in (9), an augmented state vector is formed and given by

$$\mathbf{X}(t) = \begin{bmatrix} \mathbf{x}(t) & \mathbf{x}_{SF}(t) \end{bmatrix}^T \qquad \textbf{(11)}$$

Combining (9) and (10) yields the following augmented system:

$$\begin{bmatrix} \dot{\mathbf{x}}(t) \\ \dot{\mathbf{x}}_{SF}(t) \end{bmatrix} = \begin{bmatrix} \mathbf{F}(t) & \mathbf{G}(t)\,\mathbf{H}_{SF}(t) \\ 0 & \mathbf{F}_{SF}(t) \end{bmatrix} \begin{bmatrix} \mathbf{x}(t) \\ \mathbf{x}_{SF}(t) \end{bmatrix} + \begin{bmatrix} 0 \\ \mathbf{G}_{SF}(t) \end{bmatrix} \mathbf{w}_2(t) \qquad \textbf{(12)}$$

$$\dot{\mathbf{X}}(t) = \mathbf{F}_T(t)\,\mathbf{X}(t) + \mathbf{G}_T(t)\,\mathbf{w}_2(t)$$

$$\mathbf{z}(t) = \begin{bmatrix} \mathbf{H}(t) & 0 \end{bmatrix} \begin{bmatrix} \mathbf{x}(t) \\ \mathbf{x}_{SF}(t) \end{bmatrix} + \mathbf{v}(t) = \mathbf{H}_T(t)\,\mathbf{X}(t) + \mathbf{v}(t)$$

Using Singer's model, the acceleration is uniformly distributed between $-A_{max}$ and A_{max} and the mean number of acceleration changes, α, in a unit time is distributed according to a Poisson process. This results in a first-order Markov process with variance σ^2 and time constant $1/\alpha$. The power spectral density corresponding to this exponential process is

$$\Psi(\omega) = \frac{2\sigma^2\alpha}{\omega^2 + \alpha^2} \qquad \textbf{(13)}$$

and the system transfer function for the shaping filter is

$$H(s) = \frac{\sigma\sqrt{2\alpha}}{s^2 + \alpha^2} \qquad \textbf{(14)}$$

The system model for this shaping filter is

$$\dot{\mathbf{x}}_{SF}(t) = \begin{bmatrix} -\alpha \\ -\alpha \end{bmatrix} \mathbf{x}_{SF}(t) + \begin{bmatrix} \sigma\sqrt{2\alpha} \\ \sigma\sqrt{2\alpha} \end{bmatrix} \mathbf{w}_2(t) \qquad \textbf{(15)}$$

$$\mathbf{w}_2(t) = \begin{bmatrix} 1 \end{bmatrix} \mathbf{x}_{SF}(t)$$

The augmented system then becomes

$$\begin{bmatrix} \dot{x}(t) \\ \ddot{x}(t) \\ \dot{x}_1(t) \\ \dot{y}(t) \\ \ddot{y}(t) \\ \dot{y}_1(t) \end{bmatrix} = \begin{bmatrix} 0 & 1 & 0 & 0 & 0 & 0 \\ 0 & 0 & 1 & 0 & 0 & 0 \\ 0 & 0 & -\alpha & 0 & 0 & 0 \\ 0 & 0 & 0 & 0 & 1 & 0 \\ 0 & 0 & 0 & 0 & 0 & 1 \\ 0 & 0 & 0 & 0 & 0 & -\alpha \end{bmatrix} \begin{bmatrix} x(t) \\ \dot{x}(t) \\ x_1(t) \\ y(t) \\ \dot{y}(t) \\ y_1(t) \end{bmatrix} + \begin{bmatrix} 0 & 0 \\ 0 & 0 \\ \sigma\sqrt{2\alpha} & 0 \\ 0 & 0 \\ 0 & 0 \\ 0 & \sigma\sqrt{2\alpha} \end{bmatrix} \mathbf{w}_2(t) \qquad \textbf{(16)}$$

$$\begin{bmatrix} x(t) \\ y(t) \end{bmatrix} = \begin{bmatrix} 1 & 0 & 0 & 0 & 0 & 0 \\ 0 & 0 & 0 & 1 & 0 & 0 \end{bmatrix} \begin{bmatrix} x(t) \\ \dot{x}(t) \\ x_1(t) \\ y(t) \\ \dot{y}(t) \\ y_1(t) \end{bmatrix} + \mathbf{v}(t)$$

with $\mathbf{w}_2(t)$ and $\mathbf{v}(t) \sim N(0,1)$.

2.3 Sklansky model

The Sklansky model is a Cartesian coordinate, constant velocity tracking algorithm that does not model acceleration to generate position and velocity estimates of maneuvering targets.[11] It is included here because it is an extremely simple model that tracks nonmaneuvering targets and targets with slow turn rates. The target motion is described by

$$\begin{aligned} x_{n+1} &= x_n + \mathrm{T}\dot{x}_n + \tfrac{1}{2}\mathrm{T}\ddot{x}_n + \cdots \\ \dot{x}_{n+1} &= \dot{x}_n + \mathrm{T}\ddot{x}_n \end{aligned} \qquad \textbf{(17)}$$

where

x_n = target position
$\dot{x}_n$ = target velocity
T = time interval between observations
$\ddot{x}_n$ = target acceleration

The state space representation of the Sklansky model is given by

$$\begin{aligned} \mathbf{x}_{k=1} &= \Phi_k \mathbf{x}_k + \mathbf{G}_k \mathbf{a}_k \\ \mathbf{z}_k &= \mathbf{H} x_{k=1} + \mathbf{v}_k \end{aligned} \qquad \textbf{(18)}$$

where

$$\Phi_k = \begin{bmatrix} 1 & \mathrm{T} & 0 & 0 \\ 0 & 1 & 0 & 1 \\ 0 & 0 & 1 & \mathrm{T} \\ 0 & 0 & 0 & 1 \end{bmatrix}$$

$$\mathbf{x}_k = \begin{bmatrix} x & \dot{x} & y & \dot{y} \end{bmatrix} = \begin{bmatrix} x \text{ position} & x \text{ velocity} & y \text{ position} & y \text{ velocity} \end{bmatrix}^{\mathrm{T}}$$

$$\mathbf{G} = \begin{bmatrix} \mathrm{T}^2/2 & 0 \\ \mathrm{T} & 0 \\ 0 & \mathrm{T}^2/2 \\ 0 & \mathrm{T} \end{bmatrix}$$

$$\mathbf{H} = \begin{bmatrix} 1 & 0 & 0 & 0 \\ 0 & 0 & 1 & 0 \end{bmatrix}$$

$$\mathbf{a}_k = \begin{bmatrix} u_x(k) & u_y(k) \end{bmatrix}^{\mathrm{T}}$$

= random acceleration in the x and y coordinate respectively

$\mathbf{v}_\mathrm{k}$ = scalar random measurement noise with $\mathbf{Q} \sim N(0,1)$

2.4 Helferty model

Helferty[12] develops a turn-rate model that extends the work of Singer by using a maneuvering target model that combines a constant velocity and a probability distribution on the target's turn-rate. Helferty assumes that the acceleration is independent in both the *x* and *y* coordinates and a uniform distribution on the target's turn rate with the acceleration

maneuvers exponentially correlated. This turn-rate model leads to a linear system that is represented with a third-order Markov process instead of the first-order process.

The Helferty model assumes a process noise of constant velocity and the turn-rate uniformly distributed on the interval [$-r_{max}$, r_{max}] with the turn-rate changing α times in a unit interval. The heading angle of the target is also uniformly distributed but on the interval [$-\pi$, π]. The autocorrelation function of the target acceleration in the *x* axis is

$$
\begin{aligned}
E\left[a_x(t)\,a_x(t+\tau)\right] &= E\left[v_t\,\dot{\psi}(t)\sin\psi(t)\,v_t\,\dot{\psi}(t+\tau)\sin\psi(t+\tau)\right] \\
&= v_t^2\,E\left[\dot{\psi}^2\sin\psi(t)\sin\psi(t+\tau)\right]e^{-\alpha|\tau|} \\
&= v_t^2\,E\left[\dot{\psi}^2\sin\psi(t)\sin\left(\psi(t)+\dot{\psi}\tau\right)\right]e^{-\alpha|\tau|} \\
&= v_t^2\,E\left[\dot{\psi}^2\sin\psi(t)\left(\sin\psi(t)\cos\dot{\psi}\tau+\sin\dot{\psi}\tau\cos\psi(t)\right)\right]e^{-\alpha|\tau|} \\
&= v_t^2\,E\left[\dot{\psi}^2\sin^2\psi(t)\cos\dot{\psi}\tau+\dot{\psi}^2\sin\psi(t)\sin\dot{\psi}\tau\cos\psi(t)\right]e^{-\alpha|\tau|} \\
&= v_t^2\,E\left[\dot{\psi}^2\cos\dot{\psi}\tau\right]E\left[\sin^2\psi(t)\right]e^{-\alpha|\tau|} \\
&= \frac{v_t^2}{2}E\left[\dot{\psi}^2\cos\dot{\psi}\tau\right]e^{-\alpha|\tau|}
\end{aligned}
\qquad \textbf{(19)}
$$

The autocorrelation function for the target acceleration in the *y* axis is

$$
\begin{aligned}
E\left[a_y(t)\,a_y(t+\tau)\right] &= E\left[v_t\,\dot{\psi}(t)\cos\psi(t)\,v_t\,\dot{\psi}(t+\tau)\cos\psi(t+\tau)\right] \\
&= v_t^2\,E\left[\dot{\psi}^2\cos\psi(t)\cos\psi(t+\tau)\right]e^{-\alpha|\tau|} \\
&= v_t^2\,E\left[\dot{\psi}^2\cos\dot{\psi}\tau\right]E\left[\cos^2\psi(t)\right]e^{-\alpha|\tau|} \\
&= \frac{v_t^2}{2}E\left[\dot{\psi}^2\cos\dot{\psi}\tau\right]e^{-\alpha|\tau|}
\end{aligned}
\qquad \textbf{(20)}
$$

and the cross correlation between the *x* and *y* axis can be shown to be zero.[12]

The power spectral density of the autocorrelation function of (19) and (20) is nonlinear so Helferty computes and presents a rational approximation for the linear shaping filter for the turn-rate distribution. It is given as

$$
H(s) = \frac{b_1 s^2 + b_2 s + b_3}{s^3 + a_1 s^2 + a_2 s + a_3} \qquad \textbf{(21)}
$$

The state equation and measurement model used by Helferty is the same as in (9) with

$$
\mathbf{x}(t) = \begin{bmatrix} x(t) & \dot{x}(t) & y(t) & \dot{y}(t) \end{bmatrix}^T
$$

$$
\mathbf{F}(t) = \begin{bmatrix} 0 & 1 & 1 & 0 \\ 0 & 0 & 0 & 0 \\ 0 & 0 & 0 & 1 \\ 0 & 0 & 0 & 0 \end{bmatrix}
$$

$$
\mathbf{G}(t) = \begin{bmatrix} 0 & 1 & 0 & 0 \\ 0 & 0 & 0 & 1 \end{bmatrix}^T
$$

$$
\mathbf{H}(t) = \begin{bmatrix} 1 & 0 & 0 & 0 \\ 0 & 0 & 1 & 0 \end{bmatrix}
$$

Applying the whitening process described in Section 2.1, the model for the third-order linear shaping filter given in (21) for one coordinate is

$$\dot{\mathbf{x}}_{SF}(t) = \begin{bmatrix} 0 & 1 & 0 \\ 0 & 0 & 1 \\ -a_3 & -a_2 & -a_1 \end{bmatrix} \begin{bmatrix} x_3(t) \\ x_4(t) \\ x_5(t) \end{bmatrix} + \begin{bmatrix} 0 \\ 0 \\ 1 \end{bmatrix} \mathbf{w}_2(t) \qquad (22)$$

$$\mathbf{w}_1(t) = \begin{bmatrix} b_3 & b_2 & b_1 \end{bmatrix} \begin{bmatrix} x_3(t) \\ x_4(t) \\ x_5(t) \end{bmatrix}$$

This results in the augmented state and measurement equation

$$\dot{\mathbf{X}}(t) = \begin{bmatrix} 0 & 1 & 0 & 0 & 0 & 0 & 0 & 0 & 0 & 0 \\ 0 & 0 & b_3 & b_2 & b_1 & 0 & 0 & 0 & 0 & 0 \\ 0 & 0 & 0 & 1 & 0 & 0 & 0 & 0 & 0 & 0 \\ 0 & 0 & 0 & 0 & 1 & 0 & 0 & 0 & 0 & 0 \\ 0 & 0 & -a_3 & -a_2 & -a_1 & 0 & 0 & 0 & 0 & 0 \\ 0 & 0 & 0 & 0 & 0 & 0 & 1 & 0 & 0 & 0 \\ 0 & 0 & 0 & 0 & 0 & 0 & 0 & b_3 & b_2 & b_1 \\ 0 & 0 & 0 & 0 & 0 & 0 & 0 & 0 & 1 & 0 \\ 0 & 0 & 0 & 0 & 0 & 0 & 0 & 0 & 0 & 1 \\ 0 & 0 & 0 & 0 & 0 & 0 & 0 & -a_3 & -a_2 & -a_1 \end{bmatrix} \mathbf{X}(t) + \begin{bmatrix} 0 & 0 \\ 0 & 0 \\ 0 & 0 \\ 0 & 0 \\ 1 & 0 \\ 0 & 0 \\ 0 & 0 \\ 0 & 0 \\ 0 & 0 \\ 0 & 1 \end{bmatrix} \mathbf{w}_2(t) \qquad (23)$$

$$\mathbf{z}(t) = \begin{bmatrix} 1 & 0 & 0 & 0 & 0 & 0 & 0 & 0 & 0 & 0 \\ 0 & 0 & 0 & 0 & 0 & 1 & 0 & 0 & 0 & 0 \end{bmatrix} \mathbf{X}(t) + \mathbf{v}(t)$$

where

$$\mathbf{X}(t) = \begin{bmatrix} x(t) & \dot{x}(t) & x_3(t) & x_4(t) & x_5(t) & y(t) & \dot{y}(t) & y_3(t) & y_4(t) & y_5(t) \end{bmatrix}$$

and the process noise is normally distributed with zero mean and unit variance.

2.5 Bar-Shalom and Fortmann model

Another exponentially correlated acceleration model based on the Singer Model is presented by Bar-Shalom and Fortmann[2]. They use a linear shaping filter to augment the Kalman filter. The continuous-time state equation and measurement model is

$$\dot{\mathbf{x}}(t) = \begin{bmatrix} 0 & 1 & 0 & 0 & 0 & 0 \\ 0 & 0 & 1 & 0 & 0 & 0 \\ 0 & 0 & -\alpha & 0 & 0 & 0 \\ 0 & 0 & 0 & 0 & 1 & 0 \\ 0 & 0 & 0 & 0 & 0 & 1 \\ 0 & 0 & 0 & 0 & 0 & -\alpha \end{bmatrix} \mathbf{x}(t) + \mathbf{w}(t) \qquad (24)$$

$$\mathbf{z}(t) = \begin{bmatrix} 1 & 0 & 0 & 0 & 0 & 0 \\ 0 & 0 & 0 & 1 & 0 & 0 \end{bmatrix} \mathbf{x}(t) + \mathbf{v}(t)$$

$$\mathbf{x}(t) = \begin{bmatrix} x(t) & \dot{x}(t) & \ddot{x}(t) & y(t) & \dot{y}(t) & \ddot{y}(t) \end{bmatrix}^T$$

The discrete-time state equation corresponding to (24) with sample interval T is

$$\mathbf{x}(k+1) = \mathbf{F}\,\mathbf{x}(k) + \mathbf{w}(k) \qquad (25)$$

where

$$\mathbf{F} = e^{\mathbf{A}T} = \begin{bmatrix} 1 & T & (\alpha T - 1 + e^{-\alpha T})/\alpha^2 & 0 & 0 & 0 \\ 0 & 1 & (1 + e^{-\alpha T})/\alpha^2 & 0 & 0 & 0 \\ 0 & 0 & e^{-\alpha T} & 0 & 0 & 0 \\ 0 & 0 & 0 & 1 & T & (\alpha T - 1 + e^{-\alpha T})/\alpha^2 \\ 0 & 0 & 0 & 0 & 1 & (1 + e^{-\alpha T})/\alpha^2 \\ 0 & 0 & 0 & 0 & 0 & e^{-\alpha T} \end{bmatrix}$$

The discrete-time process noise covariance matrix **Q** is given by

$$\mathbf{Q} = 2\alpha\sigma_m^2 \begin{bmatrix} T^5/20 & T^4/8 & T^3/6 & 0 & 0 & 0 \\ T^4/8 & T^3/6 & T^2/2 & 0 & 0 & 0 \\ T^3/6 & T^2/2 & T & 0 & 0 & 0 \\ 0 & 0 & 0 & T^5/20 & T^4/8 & T^3/6 \\ 0 & 0 & 0 & T^4/8 & T^3/6 & T^2/2 \\ 0 & 0 & 0 & T^3/6 & T^2/2 & T \end{bmatrix} \quad \textbf{(26)}$$

3. MODEL COMPARISONS

The five models described above where tested using Monte-Carlo simulations with 50 replications in order to compare the state estimation performance of each model. Two different target paths[12] were used in the simulations. The first was a target performing an S turn lasting 40 seconds and the second is also a S turn maneuver but with an straight segment between turns and lasts for 80 seconds. The target paths are shown in Figure 2 while Table 1 provides a summary of the maneuver parameters used in the simulations. Figure 2a is the simulated target path for the S turn without the straight segment and Figure 2b is the simulated target path for the S turn with the straight segment. The "x" denotes the starting position of the target.

The remaining model specific parameters and initial error covariance matrices needed to perform the filter simulations are as follows:

- Singer (Polar)
  $P_{\max} = 0.1$

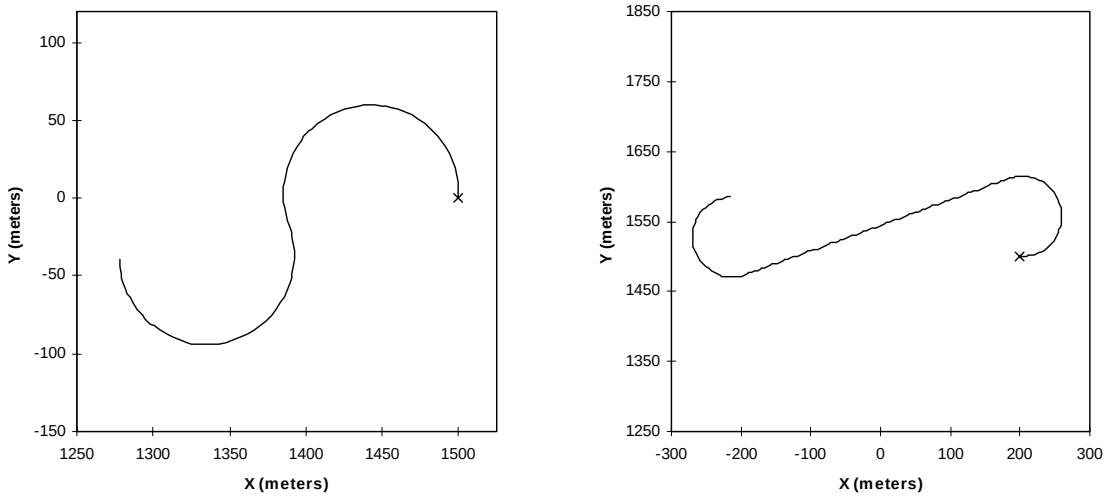

a) S turn without straight segment b) S turn with straight segment

Figure 2: Simulated Target Paths

Table 1: Kalman Filter Simulation Parameter Summary

	Scenario	
	S turn without straight segment	S turn with straight segment
Initial *x, y* position	(1500 m, 0 m)	(200 m, 1500 m)
Initial Polar position	$r = 1500$ m, $\vartheta = 0^\circ$	$r = 1513$ m, $\vartheta = 82.4^\circ$
Initial heading	90°	0°
Duration	40 sec	80 sec
Turn rate	10 m/s for 20 sec –10 m/s for 20 sec	10 m/s for 20 sec 0 m/s for 40 sec –10 m/s for 20 sec
Sample rate	$T = 0.5\ \text{s}^{-1}$	$T = 0.5\ \text{s}^{-1}$
Range measurement variance	$\sigma_r = 10\ \text{m}^2$	$\sigma_r = 10\ \text{m}^2$
Bearing measurement variance	$\sigma_\vartheta = 0.0001\ \text{rad}^2$	$\sigma_\vartheta = 0.0001\ \text{rad}^2$
Maximum acceleration	$A_{\max} = 1.745\ \text{m/s}^2$	$A_{\max} = 1.745\ \text{m/s}^2$
Forward velocity	$v_t = 10\ \text{m/s}$	$v_t = 10\ \text{m/s}$
Maximum turn rate	$r_{\max} = 0.1745\ \text{rad/s}$	$r_{\max} = 0.1745\ \text{rad/s}$
Mean number of changes	$\alpha = 0.05556\ \text{s}^{-1}$	$\alpha = 0.05556\ \text{s}^{-1}$

$P_0 = 0.4$

Q as defined in (4)

P initialized according to (7)

- Singer (Cartesian)

$$\mathbf{Q} = \begin{bmatrix} 1 & 0 \\ 0 & 1 \end{bmatrix}$$

P initialized with [100000 1000 1000 100000 1000 1000] along the main diagonal

- Sklansky

$$\mathbf{Q} = \begin{bmatrix} 1 & 0 \\ 0 & 1 \end{bmatrix}$$

P initialized with [100000 1000 100000 1000] along the main diagonal

- Helferty

$a_1 = 0.1667$, $a_2 = 0.0249$, $a_3 = 0.0010$, $b_1 = 0.2335$, $b_2 = 0.2132$, $b_3 = 0.0019$ according to Helferty's formulas[12]

$$\mathbf{Q} = \begin{bmatrix} 1 & 0 \\ 0 & 1 \end{bmatrix}$$

P initialized with [100000 1000 1000 1000 1000 100000 1000 1000 1000 1000] along the main diagonal

- Bar-Shalom and Fortmann

$\sigma_m = A_{\max}/6$

P initialized with [100000 1000 1000 100000 1000 1000] along the main diagonal

All of the models performed exceedingly well with extremely small average position and velocity errors and RMS position and velocity errors regardless of target path used. Figure 3 and Figure 4 show the average range and bearing errors, respectively, for both target paths using the Singer model in Polar coordinates. The average range errors are less than ±4 meters for either target path while the average bearing error is between ±0.3°. The average range and bearing rate errors are show in Figure 5 and Figure 6 while the RMS range and bearing errors are shown in Figure 7 and the RMS range and bearing rate errors are shown in Figure 8. The average range rate error is between ±5 m/s and the average bearing rate is

between ±0.4 deg/s. The RMS errors are 2-4 meters for range, 0.3-0.6 m/s for range rate, 0.5-2° for bearing and 0.05 deg/s for bearing rate.

The four Cartesian models and the Singer Polar model state estimate converted to Cartesian coordinates are compared next. Since the S turn path is along the 0° radial, the *x* position error is smaller (±5 m) then the y position (±20 m) for all the models. The opposite is true for the S turn with the straight segment since it is along the 90° radial. The *x* position error is between ±25 m and the *y* position error is between ±5 m. This can be seen in Figure 9 and Figure 10. With few exceptions, the average velocity error, either *x* or *y*, are between ±5 m/s. The Singer Polar model with the state estimate converted to Cartesian coordinates and the Sklansky model produce the largest velocity errors but the never exceed ±15 m/s. The average velocity errors are shown in Figure 11 and Figure 12.

The RMS errors for both position and velocity are almost indistinguishable. The *x* and *y* RMS position errors are shown in Figure 13 and Figure 14, respectively. The RMS *x* and *y* velocity errors are shown in Figure 15 and Figure 16. As expected, the Sklansky model performs the worst since it is a constant velocity model that does not include acceleration, *e.g.* acceleration treated as added noise.

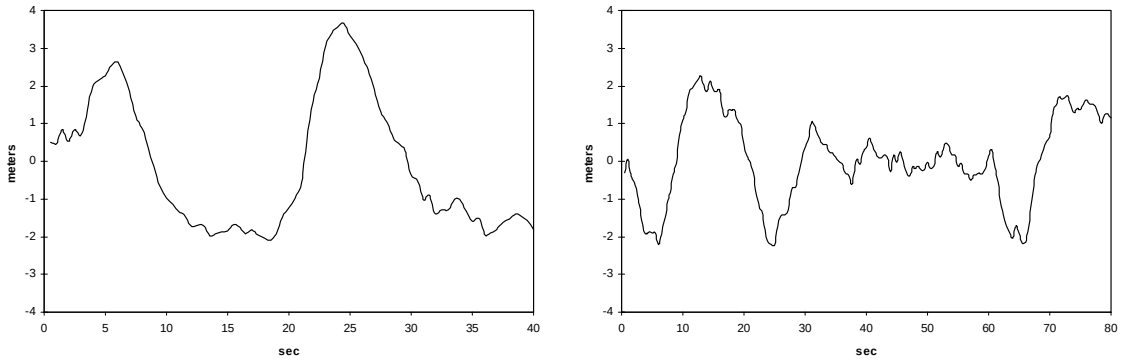

a) S turn without straight segment b) S turn with straight segment

Figure 3: Singer Model (Polar) Average Range Error

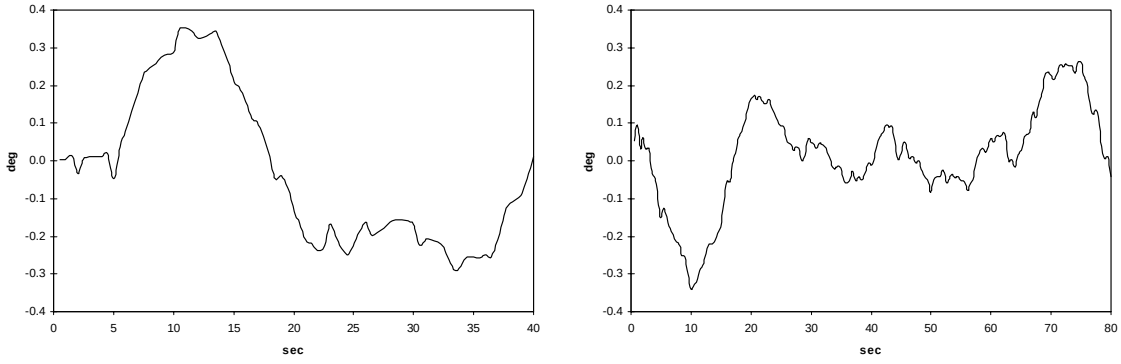

a) S turn without straight segment b) S turn with straight segment

Figure 4: Singer Model (Polar) Average Bearing Error

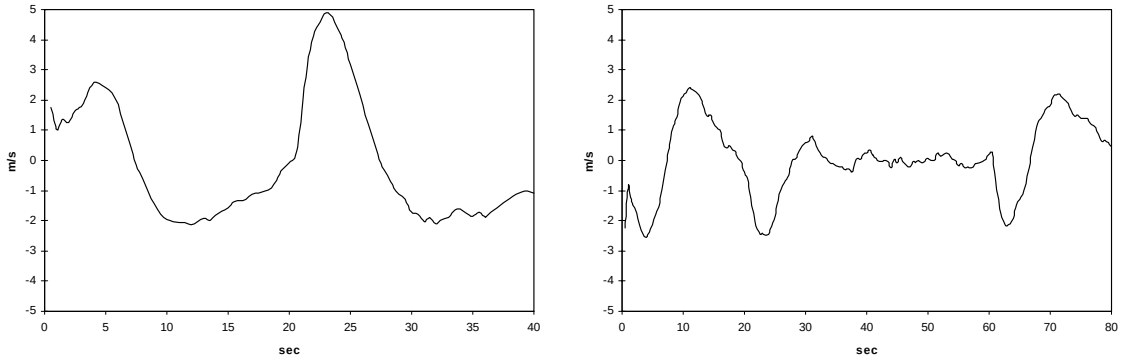

a) S turn without straight segment b) S turn with straight segment

Figure 5: Singer Model (Polar) Average Range Rate Error

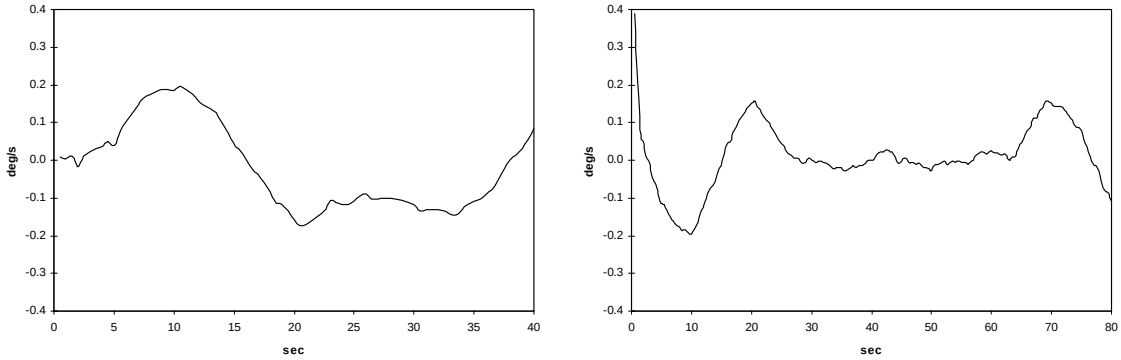

a) S turn without straight segment b) S turn with straight segment

Figure 6: Singer Model (Polar) Average Bearing Rate Error

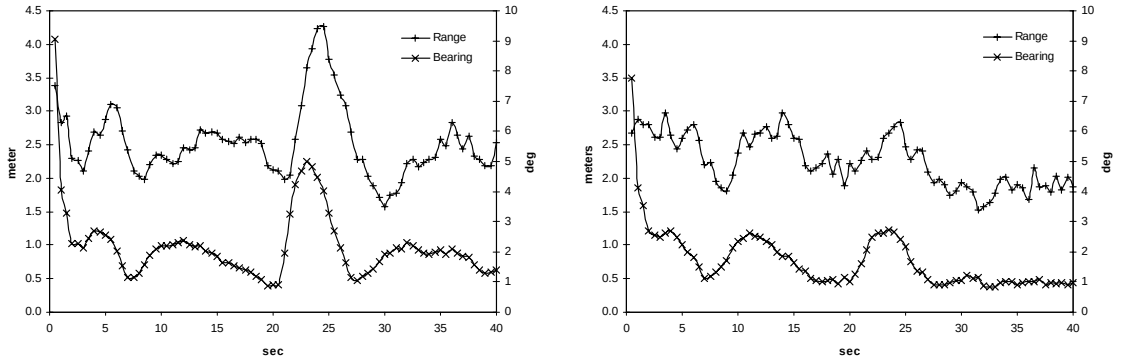

a) S turn without straight segment b) S turn with straight segment

Figure 7: Singer Model (Polar) RMS Range and Bearing Error

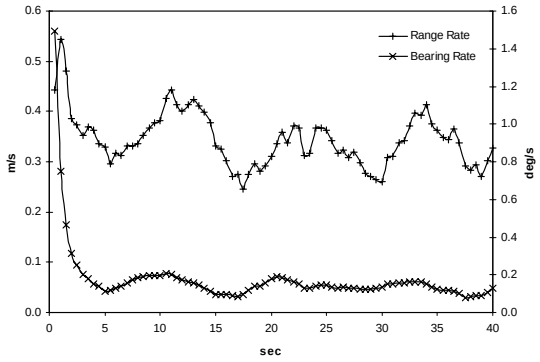

a) S turn without straight segment

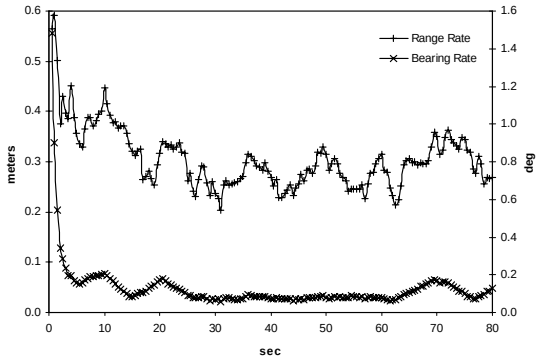

b) S turn with straight segment

Figure 8: Singer Model (Polar) RMS Range Rate and Bearing Rate Error

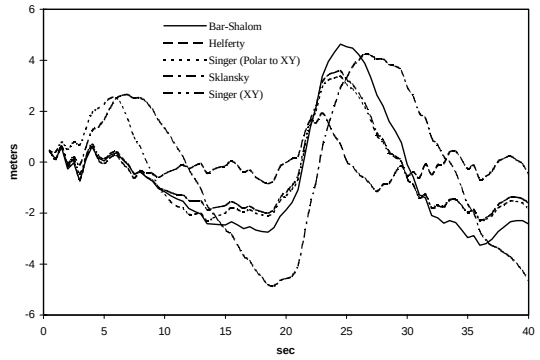

a) S turn without straight segment

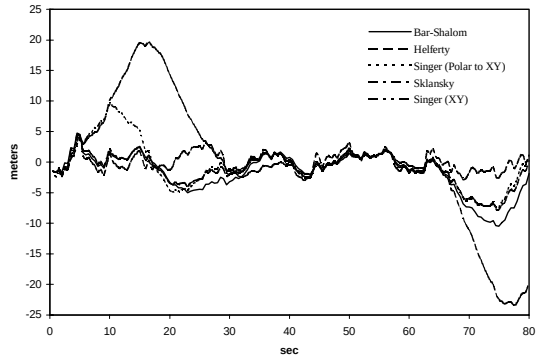

b) S turn with straight segment

Figure 9: Cartesian Models Average X Position Errors

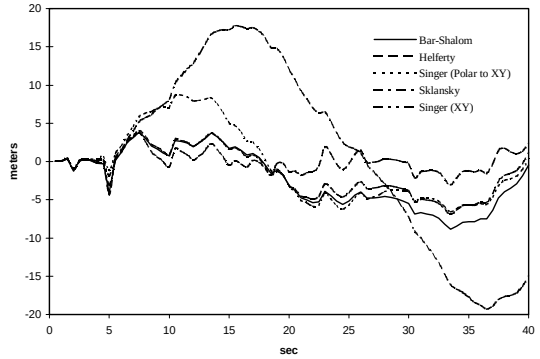

a) S turn without straight segment

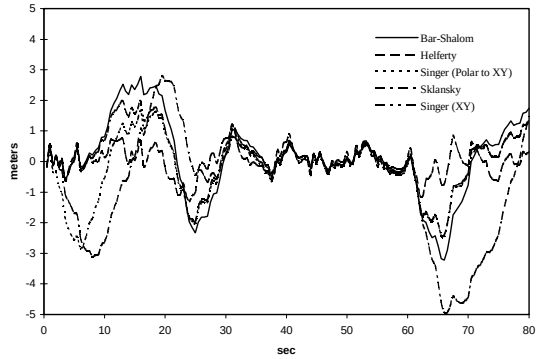

b) S turn with straight segment

Figure 10: Cartesian Models Average Y Position Errors

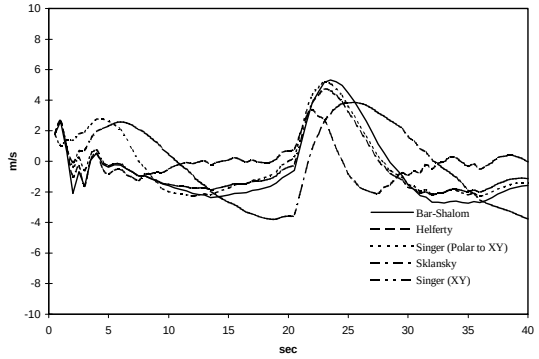

a) S turn without straight segment

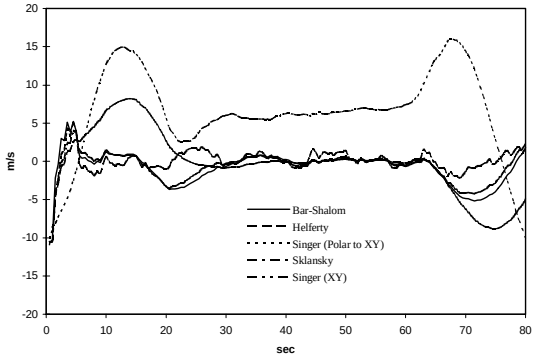

b) S turn with straight segment

Figure 11: Cartesian Models Average X Velocity Errors

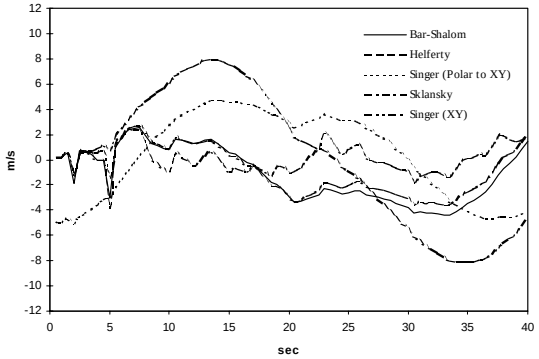

a) S turn without straight segment

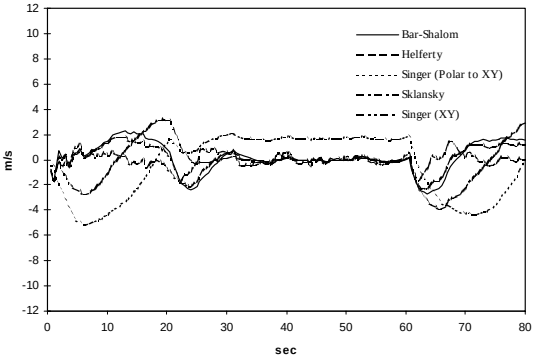

b) S turn with straight segment

Figure 12: Cartesian Models Average Y Velocity Errors

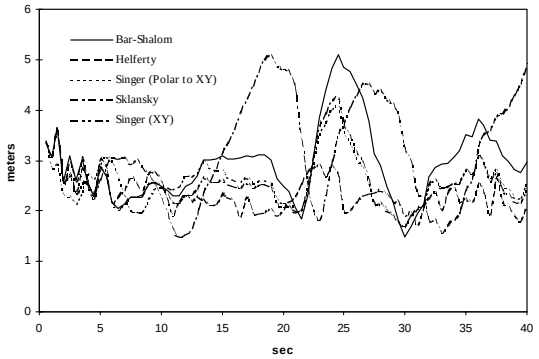

a) S turn without straight segment

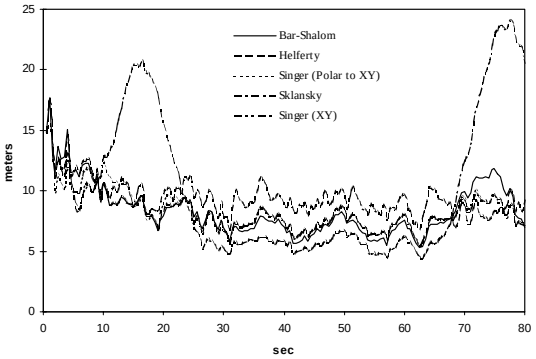

b) S turn with straight segment

Figure 13: Cartesian Models RMS X Position Errors

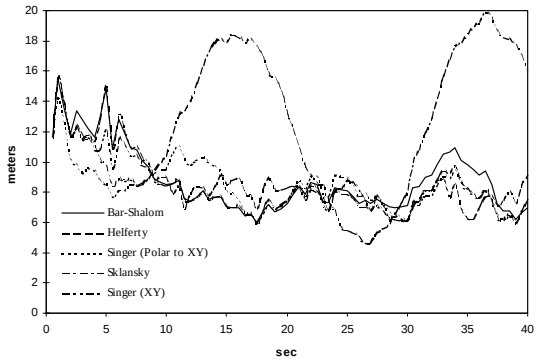

a) S turn without straight segment

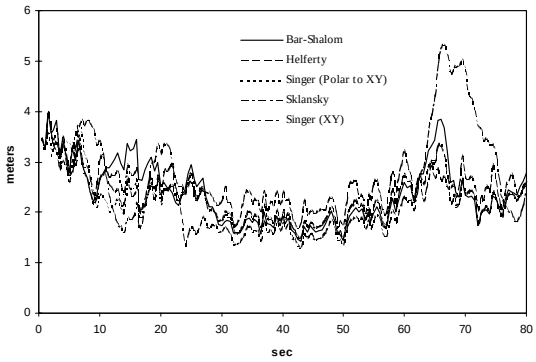

b) S turn with straight segment

Figure 14: Cartesian Models RMS Y Position Errors

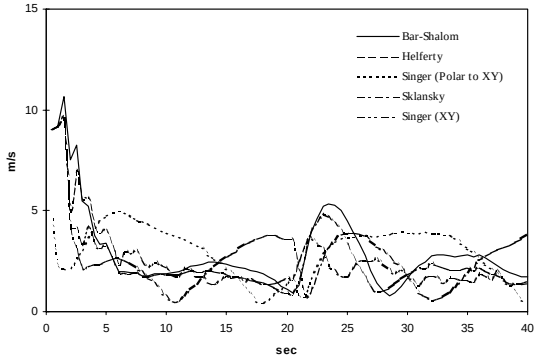

a) S turn without straight segment

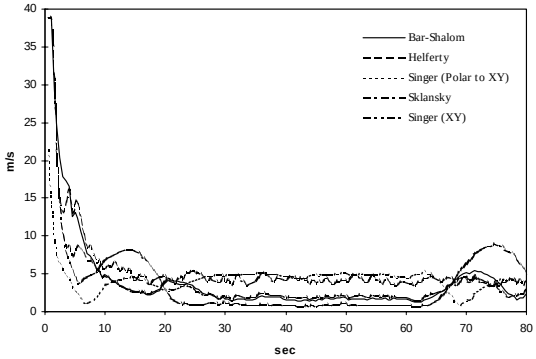

b) S turn with straight segment

Figure 15: Cartesian Models RMS X Velocity Error

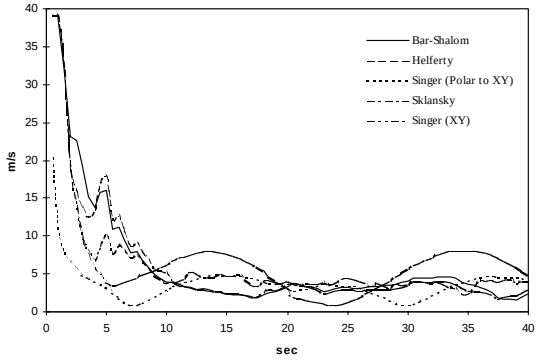

a) S turn without straight segment

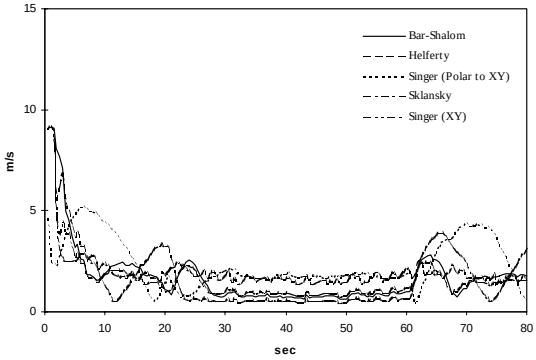

b) S turn with straight segment

Figure 16: Cartesian Models RMS Y Velocity Errors

Table 2: Maneuvering Target Model Complexity

Model	
Singer (Polar)	2270
Singer (Cartesian)	2274
Helferty	8390
Sklansky	896
Bar-Shalom and Fortmann	2946

4. SUMMARY

The exponentially correlated acceleration models appear to be valid and accurate models of target maneuvers as demonstrated above. All of the model, whether in Polar, Cartesian, or Polar converted to Cartesian provide very accurate position estimates. The only significant difference is when velocity estimates are considered due to the nonlinear conversion of the Singer Polar estimates to Cartesian estimates and the constant velocity assumption of the Sklanksy model. Besides state estimate accuracy, another consideration in choosing a maneuvering target tracking model is the computational complexity of the model. One such measure is the number of floating point operations (flops).

Table 2 shows the number of flops for one iteration of state estimate extrapolation, error covariance extrapolation, Kalman gain matrix computation, state estimate update and error covariance update for each model. The conversion of the measurement noise covariance matrix from Polar to Cartesian coordinates only add an additional 32 flops. As can be seen, the two Singer models and the Bar-Shalom and Fortmann models, each a six state estimate model, require approximately the same number of flops. The Bar-Shalom and Fortmann model requires more flops due to the size of the Q and G matrices. The Sklansky model is a four state estimator and requires about 2/3 of the number of flops of the Singer model while the Helferty model is a 10 state estimate model requiring over three times as many flops as the Singer model. The flops were computed for comparable runs of each model averaged over 80 iterations of the update process using MATLAB.

Based on the results shown in this paper, the Singer model in Cartesian coordinates or Polar coordinates with position and velocity converted to Cartesian coordinates are remarkably accurate and with limited computational burden. If increased accuracy is required, several other options are available. The simplest approach is to apply the debiasing methodology presented by Lerro and Bar-Shalom.[13] They describe a methodology for computing the measurement error covariance matrix in (2) differently that they state insures that the true measurement error statistics are used when performing the Polar to Cartesian conversion. Another possible alternative is to use the multiple model approach where multiple models are maintained simultaneously and determine which state estimate to use based upon detecting and estimating the target's maneuvering. Since the performance of the Singer model can degrade during nonmaneuvering portions of a targets trajectory, one could use two different Singer-based model filters with different values of the maneuver variance, σ_m^2, and time correlation, α, and use hypothesis testing to determine when to switch between the two models.[14] When a target is not maneuvering, the Singer model is used to track the target with $\alpha \to \infty$ and $\sigma_m^2 = 0$. Once a maneuver is detected the Singer model with a finite α and $\sigma_m^2 \neq 0$ is used. A similar approach is to use filters of different dimensions and switch between them based on maneuver detection. One such approach is the variable dimension filter of Bar-Shalom and Birmiwal[15] in which they use a four state $(x, \dot{x}, y, \dot{y})$ constant velocity model when a target is not maneuvering. Based on a maneuver detection scheme, new state components are added and a constant acceleration model with six states, $(x, \dot{x}, \ddot{x}, y, \dot{y}, \ddot{y})$, is used. Once the maneuver is complete, the four state model is used again.

Two other possible approaches which can be used to increase accuracy are the interacting multiple model (IMM) algorithm and innovations-based approach. The IMM approach consists of a set of several filters which interact through state estimate mixing to track a maneuvering target. Efe and Atherton[16] present one such example of an IMM utilizing adaptive turn rate models while Blair, *et al.*,[17] use IMM filtering based on exponentially correlated acceleration models. Blair, *et al.*, use four models in their IMM filter. They include a constant velocity, a constant acceleration, and exponentially correlated model with increasing accelerations and an exponentially correlated model with decreasing accelerations.

5. REFERENCES

1. A. Gelb (editor), *Applied Optimal Estimation*, Cambridge, Ma: M.I.T. Press, 1974

2. Y. Bar-Shalom and T. E. Fortmann, *Tracking and Data Association*, Orlando FL: Academic Press, Inc., 1988.
3. K. Spingarn and H. L. Weidemann, "Linear Regression Filtering and Prediction for Tracking Maneuvering Aircraft Targets," *IEEE Transactions on Aerospace and Electronic Systems*, vol. AES-8, no. 6, pp. 800-810, November 1972.
4. B. D. O. Anderson and J. B. Moore, *Optimal Filtering*, Englewood Cliffs, NJ: Prentice-Hall Inc., 1979.
5. F. R. Castella and F. G. Dunnebacke, "Analytical Results for the *x, y* Kalman Tracking Filter," *IEEE Transactions on Aerospace and Electronic Systems*, vol. AES-10, no. 6, pp. 891-895, November 1974.
6. S. N. Balakrishnan and J. L. Speyer, "Coordinate-Transformation-Based Filter for Improved Target Tracking," *Journal of Guidance, Control, and Dynamics*, vol. 9, no. 6, pp. 704-709, November/December 1986.
7. Singer, R. A., "Estimating Optimal Tracking Filter Performance for Manned Maneuvering Targets," *IEEE Transactions on Aerospace and Electronic Systems*, vol. AES-6, no. 4, .pp. 473-483, July 1970.
8. Singer, R. A. and K. W. Behnke, "Real-Time Tracking Filter Evaluation and Selection for Tactical Applications," *IEEE Transactions on Aerospace and Electronic Systems*, vol. AES-7, no. 1, pp. 100-110, January 1971.
9. Singer, R. A., R. G. Sea, and K. B. Housewright, "Derivation and Evaluation of Improved Tracking Filters for Use in Dense Multitarget Environments", *IEEE Transactions on Information Theory*, vol. IT-20, no. 4, pp. 423-432, July 1974.
10. M. S. Grewal and A. P. Andrews, *Kalman Filtering: Theory and Practice*, Englewood Cliffs, NJ: Prentice-Hall, Inc., 1993.
11. J. Choi, "Comparison of Sklansky and Singer Tracking Models Via Kalman Filtering," *IEEE Southeastcon '83*, Orlando, FL, April 11-14 1983, pp. 335-338.
12. J. P. Helferty, "Improved Tracking of Maneuvering Targets: The Use of Turn-Rate Distributions for Acceleration Modeling,' *IEEE Transactions on Aerospace and Electronic Systems*, vol. 32, no. 4, pp.1355-1361, October 1996.
13. D. Lerro and Y. Bar-Shalom, "Tracking with Debiased Consistent Converted Measurements Versus EKF," *IEEE Transactions on Aerospace and Electronic Systems*, vol. 29, n. 3, pp. 1015-1022, July 1993.
14. M. S. Woolfson, "An Evaluation of Manoeuver Detector Algorithms," *The GEC Journal of Research Incorporating Marconi Review*, vol. 3, no. 3, pp. 181-190, 1985.
15. Y. Bar-Shalom and K. Birmiwal, "Variable Dimension Filter for Maneuvering Target Tracking," *IEEE Transactions on Aerospace and Electronic Systems*, vol. AES-18, no. 5, pp. 621-628 September 1982.
16. M. Efe and D. P. Atherton, "Maneuvering Target Tracking Using Adaptive Turn Rate Models in The Interacting Multiple Model Algorithm," *Proceedings of the 35th Conference on Decision and Control*, vol. 2, Kobe, Japan, December 11-13 1996, pp. 3151-3156.
17. W. D. Blair, G. A. Watson, and T. R. Rice, "Tracking Maneuvering Targets With An Interacting Multiple Model Filter Containing Exponentially-Correlated Acceleration Models," *Proceedings of the Twenty-third Southeastern Symposium on System Theory*, Columbia, SC, March 10-12 1991, pp. 224-228.